

Zinc-blende—diamond order-disorder transition in metastable crystalline $(\text{GaAs})_{1-x}\text{Ge}_{2x}$ alloys

Kathie E. Newman and John D. Dow

Department of Physics, University of Illinois at Urbana-Champaign, 1110 West Green Street, Urbana, Illinois 61801

(Received 8 December 1982)

A model of a zinc-blende—diamond order-disorder transition is proposed and applied to $(\text{GaAs})_{1-x}\text{Ge}_{2x}$ substitutional crystalline alloys. In disordered Ge-rich alloys, the stable phase is one in which either Ga or As atoms can occupy nominal cation and nominal anion sites with approximately equal probabilities; in ordered GaAs-rich material, Ga (As) atoms preferentially occupy nominal cation (anion) sites. A three-component spin Hamiltonian, mean-field theory, and empirical tight-binding theory are all used in conjunction to predict equilibrium phase diagrams and the dependence on alloy composition x of the direct band-gap energy $E_0(x)$. The theory accounts for the observed V -shaped dependence of $E_0(x)$ in $(\text{GaAs})_{1-x}\text{Ge}_{2x}$ and for several qualitative facts concerning the growth of these interesting metastable crystalline alloys.

I. INTRODUCTION

The possibility of tailoring band gaps and other properties of semiconductors for specific devices has motivated experimental attempts to fabricate new semiconductor alloys. Greene *et al.* have now successfully grown two differing (100)-oriented metastable alloys of group-IV elements with III-V compounds,¹ $(\text{GaAs})_{1-x}\text{Ge}_{2x}$,² and $(\text{GaSb})_{1-x}\text{Ge}_{2x}$,³ for all compositions x . They found for $(\text{GaAs})_{1-x}\text{Ge}_{2x}$ (Ref. 4) that the direct gap E_0 as a function of x does not exhibit conventional bowing, that is, is not parabolic in shape. As seen in Fig. 1, their data for the band gap of $(\text{GaAs})_{1-x}\text{Ge}_{2x}$ are better represented by two straight lines that intersect with a V shape, namely with a discontinuous slope at a special composition x_c (≈ 0.3). Moreover, the absorption coefficient changes abruptly near $x = x_c$, with the sharp edge for GaAs-rich $x < x_c$ becoming suddenly "softer" for $x \geq x_c$.⁴ It was proposed⁴ that there is a phase transition for $x = x_c$: The composition ranges $x < x_c$ and $x > x_c$ would then be different phases of the alloy, each having different electronic properties.

Here we model the proposed order-disorder phase transition,⁵ and discuss its consequences for the electronic structure of the alloy $(\text{GaAs})_{1-x}\text{Ge}_{2x}$. We suggest that there are both zinc-blende (as in GaAs) and diamond (Ge) phases of the alloy that are separated by a transition at $x = x_c$. Both zinc-blende and diamond lattices are face-centered-cubic lattices with a two-atom basis.⁶ However, the zinc-

blende lattice is of lower symmetry than the diamond lattice due to the existence of distinct anion and cation sites; the diamond lattice is a nominal zinc-blende structure whose nominal anions and

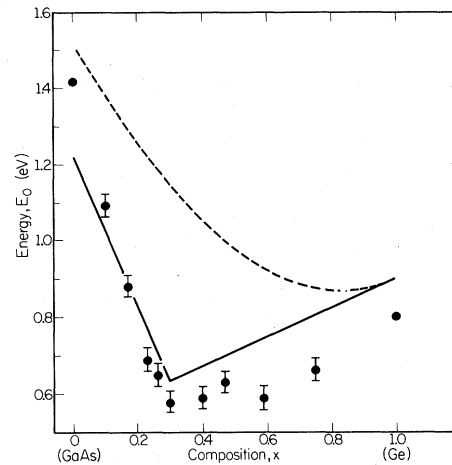


FIG. 1. Experimental data for the direct gap in $(\text{GaAs})_{1-x}\text{Ge}_{2x}$ alloys compared with mean-field theory (solid curve) and the conventional virtual-crystal approximation (Refs. 18 and 19) (dashed curve) (after Ref. 4). The mean-field theory postulates a zinc-blende—diamond order-disorder phase transition at $x_c = 0.3$. This theory allows for the existence of many antisite defects even for $x = 0$, lowering the band gap E_0 . Furthermore, note that both theories use 4-K empirical tight-binding parameters, while experimental data are taken at room temperature, where the band gaps are smaller.

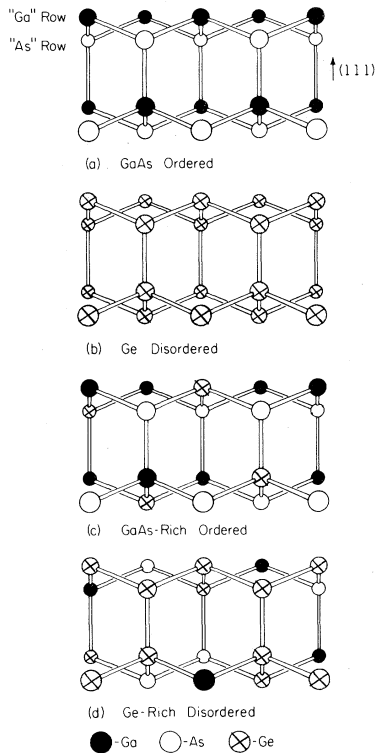


FIG. 2. Schematic model of the phases of $(\text{GaAs})_{1-x}\text{Ge}_{2x}$ alloys: (a) GaAs (ordered zinc-blende structure), (b) Ge (disordered) diamond structure, (c) GaAs-rich ordered zinc-blende structure of the alloy, and (d) Ge-rich disordered diamond structure of the alloy, after Ref. 4. Note that the zinc-blende lattice [(a) and (c)] is an *ordered* structure in that virtually all Ga atoms (dark circles) and As atoms (empty circles) are found on their correct nominal sites ("Ga" and "As" rows, respectively), while the presence of as many "antisite" as "on-site" defects in (d) indicates a *disordered* diamond lattice.

nominal cations are both the same (e.g., Ge). This nominal zinc-blende lattice may be occupied in this alloy in either of two different ways (see Fig. 2).

(1) In the GaAs-rich *ordered* zinc-blende phase [Fig. 2(c)], virtually all Ga atoms (dark circles) occupy nominal Ga sites ("Ga" rows) and virtually all As atoms (empty circles) occupy nominal As sites ("As" rows), with Ge atoms (shaded circles) dispersed randomly on either site.

(2) In the *disordered* diamond phase stable for Ge-rich material [Fig. 2(d)], there are as many "antisite" as "on-site" atoms in the nominal zinc-blende lattice, namely Ga atoms (dark circles) on nominal-As sites ("As" rows) and As atoms (empty circles)

TABLE I. For $x < x_c$, average occupancies of the nominal "Ga" and "As" sublattices by atoms Ga, As, and Ge in terms of composition x and the order parameter M .

	"Ga"	"As"
$\langle P_{\text{Ga}} \rangle$	$(1-x+M)/2$	$(1-x-M)/2$
$\langle P_{\text{As}} \rangle$	$(1-x-M)/2$	$(1-x+M)/2$
$\langle P_{\text{Ge}} \rangle$	x	x

on nominal-Ga sites ("Ga" rows).

The zinc-blende structures of Figs. 2(a) and 2(c) are referred to as *ordered* since, on the average, Ga and As atoms are found on the correct nominal sublattices. The diamond structure of Figs. 2(b) and 2(d) will similarly be referred to as *disordered*: On the average, there is *not* a distinction between "Ga" and "As" rows.

To treat the order-disorder transition between these two types of phases, we first define the order parameter of the transition in terms of the average sublattice occupancies of each type of atom. For example, we define $\langle P_{\text{Ga}} \rangle_{\text{"Ga"}}$ ($\langle P_{\text{As}} \rangle_{\text{"Ga"}}$) to be the average occupancy of Ga (As) atoms on the nominal Ga sublattice ("Ga") [the theory is applicable⁷ to any zinc-blende-to-diamond alloy; not just $(\text{GaAs})_{1-x}\text{Ge}_{2x}$]. Then the order parameter M is, to first approximation,⁸ defined

$$M \equiv \langle P_{\text{Ga}} \rangle_{\text{"Ga"}} - \langle P_{\text{Ga}} \rangle_{\text{"As"}}. \quad (1.1)$$

The order parameter can assume any values from $x-1$ to $1-x$. The physical interpretation of the order parameter M can be seen as follows: If all the Ga atoms occupy nominal Ga sites, then we have $M=1-x$; if the Ga atoms are distributed evenly over nominal Ga and nominal As sites, then we have $M=0$; if all Ga atoms are on the nominal As site, then the order parameter is $M=x-1$. Thus M has an amplitude $1-x$, and is up (+) or down (-) if the Ga is ordered (either almost all on "Ga" sites or on "As" sites), but zero if the Ge is randomly distributed. In this model, we also have

$$M = \langle P_{\text{As}} \rangle_{\text{"As"}} - \langle P_{\text{As}} \rangle_{\text{"Ga"}}. \quad (1.2)$$

If we have $|M| \neq 1-x$, then some anions and cations are found on nominally "wrong" sublattice sites. This fact can be used to construct a table of average occupancies for $x < x_c$, Table I. For $x > x_c$, the disordered Ge-rich diamond-lattice phase, there is not a distinction between anion and cation sites and we have $M=0$. The average occupancies of this phase are those given by Table I, but with $M=0$: all atoms in alloys $(\text{GaAs})_{1-x}\text{Ge}_{2x}$ occupy lattice sites with probabilities determined simply by the atoms'

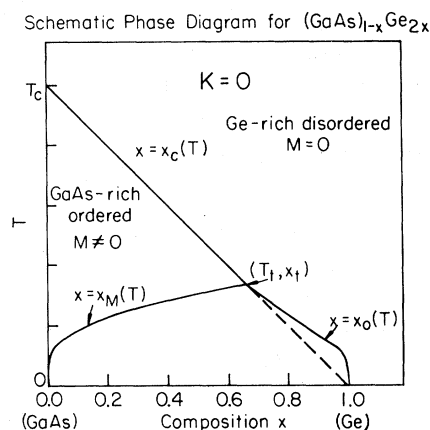


FIG. 3. For $K = 0$ [see Eq. (2.6b)], the calculated phase diagram of a $(\text{GaAs})_{1-x}\text{Ge}_{2x}$ alloy as a function of temperature T and composition x .

concentrations. Note that for $x=0$ and $M = \pm 1$ (Table I), we recover the expected zinc-blende lattice structure of GaAs, and similarly, for $x=1$ ($M=0$), we recover the diamond-lattice structure of Ge. The order parameter M is a quantity that is nonzero only in the ordered (zinc-blende) phase, $x < x_c$.

A difficulty in studying the phase transitions of the crystalline $(\text{GaAs})_{1-x}\text{Ge}_{2x}$ alloys grown by Greene *et al.* is that they are *metastable*, that is, grown under *nonequilibrium* conditions.^{1-4,9,10} Furthermore, the zinc-blende—diamond order-disorder transition discussed here does not seem to occur for most $(\text{III-V})_{1-x}\text{IV}_{2x}$ alloys grown at equilibrium, a fact that must be explained. Rather, for low temperatures, the equilibrium phase diagram of $(\text{GaAs})_{1-x}\text{Ge}_{2x}$ shows a miscibility gap (that is, the alloy phase separates into GaAs-rich and Ge-rich materials), and, for high temperatures, the alloy melts.¹¹ The growth of the metastable alloys (for all compositions x) is facilitated by secondary Ar ion bombardment, which apparently both mixes (randomly) all individual atoms and sputters away clumps of GaAs-rich or Ge-rich materials. The ion bombardment affects only the top four or so layers; the lowest of these layers of the alloy is quenched as additional layers grow above it. Once the metastable alloy is formed, its lifetime is of the order of 10^{29} y at room temperature^{3,12}; this is probably due to the small self-diffusion constants characteristic of all III-V materials.³ The growth conditions are thus designed to *inhibit* phase separation.

In order to circumvent the problems posed by the nonequilibrium nature of these alloys, we introduce the notion of equilibrium time scales, arguing that

the possible phases of the metastable alloy must be the same as those for an alloy grown at equilibrium. However, in the metastable alloy, certain of these phases are forbidden from forming by the growth conditions. Any fluid alloy grown for a composition x in the miscibility gap will, as it cools, phase separate; the zinc-blende-rich phase will simultaneously undergo an ordering transition. Phase separation, on a scale noticeable experimentally, can be inhibited if the crystal is quickly quenched in the highly mixed (due to secondary ion bombardment) state. This is because phase separation involves movement of ions or atoms over lengths the size of the domains seen experimentally (30 Å) (Ref. 13) and, for typical self-diffusion constants of As in GaAs,¹⁴ takes on the order of a day at sample-preparation temperatures (≥ 900 K, the substrate temperature). Thus phase separation does not occur in these metastable materials, which are prepared in less than a day. This argument also explains why the zinc-blende—diamond order-disorder phase transition is less easily inhibited experimentally: The question of an ordered versus disordered state can be settled by simple interchanges of nearest-neighbor atomic pairs on a scale of 3 Å, and occurs on a time scale of order minutes.¹⁵ Thus we shall execute a calculation of the *equilibrium* phase diagram, but do it in such a way that phase separation, which occurs on a time scale of order hours, can be discarded.

These ideas can be formulated in terms of a typical equilibrium phase diagram (see Figs. 3 and 4) of temperature T versus composition x . Derivation of these phase diagrams for a particular Hamiltonian (three-component spin model) and technique (mean-field theory) will be discussed in the next section and in Appendix A; here we concentrate on those qualitative features of the phase diagram which are general. Since GaAs and Ge are immiscible, we assume that energetics favor Ga atoms being adjacent to As atoms and Ge adjacent to Ge, so the equilibrium ground state at zero temperature is phase-separated pure GaAs and Ge. As temperature is increased and entropy becomes important, the stable phases are GaAs with a small concentration of Ge and Ge with a small concentration of GaAs. The solubility of the minority species in the separated phases increases with temperature until, at some temperature T (assuming the material does not melt and the zinc-blende—diamond structure is retained) the miscibility gap goes to zero. Thus the phase diagram must include a miscibility curve that increases from zero at $x=0$ to a maximum [the curve $x_M(T)$ in Figs. 3 and 4, and $x_1(T)$ in Fig. 4] and then decreases to zero at $x=1$ [curves $x_2(T)$ and $x_0(T)$]. [The miscibility gap is the length of a horizontal line intersecting both segments of this curve, e.g.,

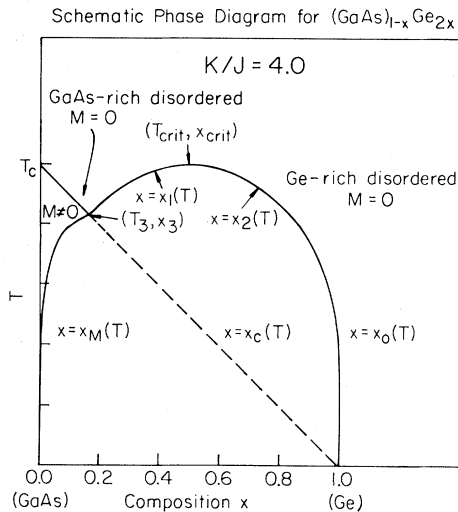


FIG. 4. For $K/J=4$, the calculated phase diagram of a $(\text{GaAs})_{1-x}\text{Ge}_{2x}$ alloy as a function of temperature T and composition x . Both this phase diagram and that of Fig. 3 should be regarded as schematic, since the theory is a mean-field theory and also does not allow for melting. If this diagram were literally the phase diagram for $(\text{GaAs})_{1-x}\text{Ge}_{2x}$, then $x_c(T_{\text{eff}})=0.3$ for $T=T_{\text{eff}}$ would fall on the dashed line and hence be a metastable solution of Eq. (2.11) (in contrast to Fig. 3).

$x_0(T) - x_M(T)$.] At very high temperatures (assuming melting does not intervene) the completely mixed and disordered phase must occur at all compositions x (even for pure GaAs); in this phase, Ga, As, and Ge atoms randomly occupy all sites with probabilities depending exclusively on their concentrations. As the temperature is lowered, first for GaAs and then for alloys $(\text{GaAs})_{(1-x)}\text{Ge}_{2x}$, this disordered high-temperature gas of atoms on lattice points must order, with the Ga atoms preferentially occupying Ga sites (surrounded by As) and the As atoms occupying As sites. The curve $x_c(T)$ forms the boundary between the ordered and disordered phases. In pure Ge ($x=1$), a zinc-blende—diamond order-disorder transition is not possible because there are neither distinct anions nor cations; hence, we must have $0 < x_c(T=0) \leq 1$. In the present model, which does not include percolation effects, we have $x_c(T=0)=1$. In general, the order-disorder transition boundary of the phase diagram, $x_c(T)$, will intersect the miscibility curve [$x_M(T)$, $x_1(T)$, $x_2(T)$, and $x_0(T)$] at a temperature T with one of two possible topologies: in Fig. 4, the miscibility gap goes to zero at an ordinary critical point, $T=T_{\text{crit}}$, and, in Fig. 3, at a special point that is (historically) labeled a tricritical point, $T=T_t$.¹⁶

The details of the phase diagram depend upon such experimental parameters as the relative strengths of the energies of interactions of Ga atoms with Ga, As, and Ge atoms. Thus, there are (at least) *two* types of nonmelting transitions that are important for these alloys: phase-separation and order-disorder. And, as shown in Fig. 4, there can be a range of temperatures $T_3 < T < T_{\text{crit}}$ at which both types of transitions can occur (for some x). [Note, however, that the order-disorder transition has not been seen *experimentally for equilibrium* $(\text{III-V})_{1-x}\text{V}_{2x}$, presumably because the melting-transition temperature is less than T_3 or T_t .] Finally, note that for low temperatures, $T < T_t$ (Fig. 3) or $T < T_3$ (Fig. 4), the phase-separation transition “masks” the (dashed) order-disorder transition. Thus, at a composition x such that the alloy phase-separates, the resulting GaAs-rich phase also orders and the Ge-rich phase also disorders. The order-disorder transition thus persists unobserved in the equilibrium phase-separated material and continues (shown by the dashed line) in the forbidden region of the phase diagram. In the metastable alloy, we propose that it is the “unmasked” order-disorder phase transition that is seen experimentally.

With a mean-field theory of the order-disorder transition of metastable $(\text{GaAs})_{1-x}\text{Ge}_{2x}$ alloys, we can calculate the alloy’s electronic properties. Specifically, results for the order parameter are input to an empirical tight-binding theory¹⁷ and to a generalized mean-field and virtual-crystal approximation in order to determine the alloy’s band structure. The success of our theory is seen in Fig. 1, where we compare our results for the direct gap E_0 as a function of x with experimental data. Further results for the band gaps as functions of x are found in Fig. 5 (mean-field theory) and compared with the predictions of the virtual-crystal model^{18,19} (Fig. 6).

This paper is organized as follows. A three-component spin model for the alloy is introduced in Sec. II, and a derivation of the order parameter M of Eqs. (1.1) and (1.2) is discussed. Details of the calculation of the phase diagram are found in Appendix A. Discussion of the calculation of band structure is found in Sec. III and Appendix B. Conclusions are presented in Sec. IV.

II. THREE-COMPONENT SPIN MODEL AND EQUILIBRIUM PHASE DIAGRAMS

Here we propose a three-component spin model for the equilibrium phase transitions of $(\text{GaAs})_{1-x}\text{Ge}_{2x}$. This model has two advantages. First, it is simple—it contains the minimum number of physical parameters necessary to obtain both

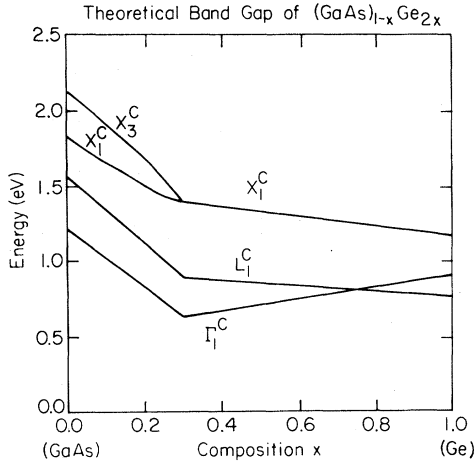


FIG. 5. Conduction-band edges, as functions of x in $(\text{GaAs})_{1-x}\text{Ge}_{2x}$, relative to the valence-band maximum, at Γ_1^C , L_1^C , X_1^C , and X_3^C points of the Brillouin zone. These were calculated using the modified mean-field virtual-crystal approximation, assuming that a zinc-blende-diamond order-disorder phase transition occurs for $x_c=0.3$.

order-disorder and phase-separation transitions. Namely, we include as parameters only six nearest-neighbor energies of interaction J_{ij} (e.g., $J_{\text{Ge-Ge}}$, $J_{\text{Ge-Ga}}$, etc.) and three chemical potentials μ_{Ga} , μ_{As} , and μ_{Ge} . We neglect for now all interactions of the substrate with the crystal, we assume that there are exactly as many Ga as As atoms, that there are not vacancies, that atoms only occupy lattice sites, that there are not structural phase transitions, and that the crystal does not melt as the temperature is increased. A second reason for studying a three-component spin model of the alloys is that similar spin models have been extensively studied. A three-component spin model was proposed originally for the study of $^3\text{He-}^4\text{He}$ mixtures²⁰; since then, three-component spin models have been applied to binary and ternary mixtures of fluids,²¹ and, more recently, to the melting of a binary alloy.²²

The alloy $(\text{GaAs})_{1-x}\text{Ge}_{2x}$ is modeled as a lattice gas. That is, an ideal zinc-blende lattice is divided into nominal "Ga" and nominal "As" sites, and each site is assumed to be singly occupied by a Ga,

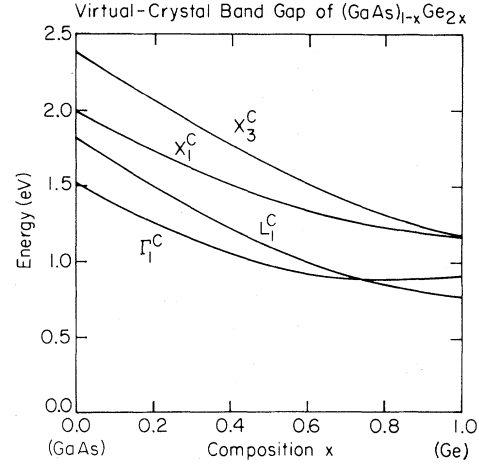


FIG. 6. Conduction-band edges, as functions of x in $(\text{GaAs})_{1-x}\text{Ge}_{2x}$, relative to the valence-band maximum, at Γ_1^C , L_1^C , X_1^C , and X_3^C points of the Brillouin zone. These were calculated using the conventional virtual-crystal approximation (Refs. 18 and 19).

As, or Ge atom. The three components of a discrete spin variable S are associated with each type of atom: $S = +1$ (Ga), 0 (Ge), and -1 (As). Thus GaAs is an "antiferromagnet," having alternating "up" (Ga) and "down" (As) spins at each site.²³ The role of the Ge in the metastable alloy, then, is to dilute the antiferromagnet with "spin-0" atoms. (The present model thus differs from the Blume-Emery-Griffiths model of $^3\text{He-}^4\text{He}$ superfluid-normal-fluid transitions,²⁰ which employ "ferromagnetic" couplings.)

Using spin S , projection operators such as $P_{\text{Ga}}(S_i)$ are defined so that $P_{\text{Ga}}(S_i)$ is either unity (if site i is occupied by a Ga atom) or zero (unoccupied). These operators are given by

$$\begin{aligned} P_{\text{Ga}}(S_i) &= S_i(S_i + 1)/2, \\ P_{\text{Ge}}(S_i) &= 1 - S_i^2, \\ P_{\text{As}}(S_i) &= S_i(S_i - 1)/2. \end{aligned} \quad (2.1)$$

This allows us to define simply a lattice-gas spin Hamiltonian H ,

$$\begin{aligned} H &= J_{\text{Ga-Ga}} \sum_{i,j} P_{\text{Ga}}(S_i)P_{\text{Ga}}(S_j) + J_{\text{As-As}} \sum_{i,j} P_{\text{As}}(S_i)P_{\text{As}}(S_j) - J_{\text{Ga-As}} \sum_{i,j} [P_{\text{Ga}}(S_i)P_{\text{As}}(S_j) + P_{\text{As}}(S_i)P_{\text{Ga}}(S_j)] \\ &\quad - J_{\text{Ga-Ge}} \sum_{i,j} [P_{\text{Ga}}(S_i)P_{\text{Ge}}(S_j) + P_{\text{Ge}}(S_i)P_{\text{Ga}}(S_j)] - J_{\text{As-Ge}} \sum_{i,j} [P_{\text{As}}(S_i)P_{\text{Ge}}(S_j) + P_{\text{Ge}}(S_i)P_{\text{As}}(S_j)] \\ &\quad - J_{\text{Ge-Ge}} \sum_{i,j} P_{\text{Ge}}(S_i)P_{\text{Ge}}(S_j) - \mu_{\text{Ga}} \sum_i P_{\text{Ga}}(S_i) - \mu_{\text{As}} \sum_i P_{\text{As}}(S_i) - \mu_{\text{Ge}} \sum_i P_{\text{Ge}}(S_i) \end{aligned} \quad (2.2)$$

(where the sum i,j is taken over nearest-neighbor pairs), a partition function Z ,

$$Z = \text{Tr} \exp[-H/(k_B T)], \quad (2.3)$$

and a free energy F ,

$$F = -(k_B T) \ln Z, \quad (2.4)$$

where k_B is Boltzmann's constant. Note that the Ga-Ga and the As-As interactions are taken to be repulsive, but all others are attractive. Using definitions (2.1), the spin Hamiltonian can be rewritten in terms of the three-component spin (with a constant term subtracted out):

$$H = J \sum_{i,j} S_i S_j - K \sum_{i,j} S_i^2 S_j^2 + L \sum_{i,j} (S_i^2 S_j + S_i S_j^2) + h \sum_i S_i + \Delta \sum_i S_i^2, \quad (2.5)$$

where we have

$$J = (J_{\text{Ga-Ga}} + J_{\text{As-As}})/4 + J_{\text{Ga-As}}/2, \quad (2.6a)$$

$$K = -(J_{\text{Ga-Ga}} + J_{\text{As-As}})/4 + J_{\text{Ga-As}}/2 - J_{\text{Ga-Ge}} - J_{\text{As-Ge}} + J_{\text{Ge-Ge}}, \quad (2.6b)$$

$$L = (J_{\text{Ga-Ga}} - J_{\text{As-As}})/4 + (J_{\text{Ga-Ge}} - J_{\text{As-Ge}})/2, \quad (2.6c)$$

$$h = z(J_{\text{As-Ge}} - J_{\text{Ga-Ge}}) + \mu_{\text{As}} - \mu_{\text{Ga}}, \quad (2.6d)$$

$$\Delta = z(2J_{\text{Ge-Ge}} - J_{\text{As-Ge}} - J_{\text{Ga-Ge}}) - \mu_{\text{As}} - \mu_{\text{Ga}} + 2\mu_{\text{Ge}}, \quad (2.6e)$$

and z is the lattice coordination number (4 for zinc blende). We use the sign convention that all J 's are positive.

Note the meaning of the terms in the three-component spin Hamiltonian, Eq. (2.5). Interaction J , Eq. (2.6a), is the term that prefers to place Ga atoms next to As atoms. That is, $S = +1$ (Ga) is aligned preferentially adjacent to $S = -1$ (As). J is thus an antiferromagnetic coupling and is positive. The sign of K , Eq. (2.6b), is less obvious. If K is negative, then there would be a tendency (for $J=0$) to form the phase-separated materials GaGe and GeAs.²⁴ It seems likely, however, that $J+K > 0$, where

$$J + K = (J_{\text{Ga-As}} - J_{\text{Ga-Ge}}) + (J_{\text{Ge-Ge}} - J_{\text{Ge-As}}). \quad (2.7)$$

That is, $J + K > 0$ implies that the system prefers to form GaAs and Ge to GaGe and GeAs compounds. The quantities h and Δ are primarily important as chemical-potential differences. Δ is thermodynamically

conjugate to the composition x , while h is conjugate to an order parameter Q that is nonzero only if there are phase-separated materials such as GaGe or GeAs [see definition (A8)]. Note that h is *not* an ordering field. (Our model does not include the staggered magnetic field, which is the ordering field for antiferromagnetic models.) The term L has an effect like a magnetic field. Since L is made up of differences of terms that are probably of the same magnitude, we argue that L (to first approximation) may be set to zero (and leave the effects of small nonzero values of L to further refinements of this theory).

Here we use a generalized definition of the order parameter M of Ga and As atoms on sublattices "Ga" and "As" (Ref. 8):

$$M \equiv (\langle P_{\text{Ga}} \rangle_{\text{Ga}} - \langle P_{\text{Ga}} \rangle_{\text{As}} + \langle P_{\text{As}} \rangle_{\text{As}} - \langle P_{\text{As}} \rangle_{\text{Ga}}) / 2. \quad (2.8)$$

Calculation of the order parameter M proceeds as follows. (Details and references will be found in Appendix A.) First, we calculate the free energy F , Eq. (2.4), in a mean-field approximation. This is done variationally²⁵: a trial form for F is found and minimized with respect to its parameters, producing an equation of the Curie-Weiss form for M [see Eq. (A15)]:

$$\frac{JzM}{k_B T} = \tanh^{-1} \frac{M}{1-x}. \quad (2.9)$$

This equation is formally equivalent to that of the Blume-Emery-Griffiths model, and is solved numerically for M as a function of x and T (Fig. 7). The

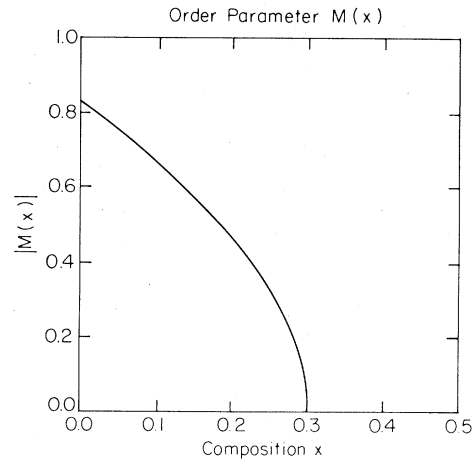


FIG. 7. Absolute value of the order parameter $M(x)$ for $(\text{GaAs})_{1-x}\text{Ge}_{2x}$, computed assuming a constant sample-preparation temperature.

TABLE II. Empirical tight-binding matrix elements of the sp^3s^* Hamiltonian in eV. Here $c = \text{Ga}$ or Ge and $a = \text{As}$ or Ge for GaAs and Ge, respectively, and a' (c') is the second neighbor of atom a (c). The parameters $E(s^*,c)$ and $E(s^*,a)$ for GaAs are the same as obtained in Ref. 17, and all parameters for Ge are the same as used in Ref. 27.

	GaAs	Ge
$E(s,c)$	-2.6713	-5.8800
$E(s,a)$	-8.3593	-5.8800
$E(p,c)$	3.6690	1.6100
$E(p,a)$	1.0410	1.6100
$E(s^*,c)$	6.7386	6.3900
$E(s^*,a)$	8.5914	6.3900
$V(s,s)$	-6.4342	-6.7800
$V(x,x)$	1.9543	1.6100
$V(x,y)$	5.0777	4.9000
$V(sc,pa)$	5.2671	4.9617
$V(sa,pc)$	4.2485	4.9617
$V(s^*c,pa)$	4.7525	4.5434
$V(s^*a,pc)$	4.2547	4.5434
$\epsilon(sa,p_x a')$	-0.21	0.0
$\epsilon(sc,p_x c')$	-0.21	0.0
$\epsilon(p_x a, p_y a')$	0.0	0.157
$\epsilon(p_x c, p_y c')$	0.0	0.157

critical-transition line, $x_c(T)$, is the locus of points that demarks solutions $M=0$ (the disordered high-temperature large- x diamond phase) from $M \neq 0$ (the ordered low-temperature small- x zinc-blende phase). That is, $x_c(T)$ is found by equating derivatives with respect to M of left- and right-hand sides of Eq. (2.9) for $M=0$; hence we have

$$k_B T_{\text{eff}} = Jz [1 - x_c(T_{\text{eff}})]. \quad (2.10)$$

This result is plotted in Figs. 3 and 4. Here T_{eff} is the *effective* (unknown) sample-preparation temperature. If this temperature is assumed to be a constant, then Eqs. (2.9) and (2.10) may be solved for the order parameter $M(x)$, provided x_c is known:

$$\frac{M}{1-x} = \tanh \frac{M}{1-x_c}. \quad (2.11)$$

In this paper, we take $x_c=0.3$, the experimental value for $(\text{GaAs})_{1-x}\text{Ge}_{2x}$.⁴ Equation (2.11), plus Table I (which relates M to sublattice occupation probabilities), are the central results of this paper.

Discussion of the calculation of the phase-separation curves, and other details of the phase diagram for different ratios of J to K , will be found in Appendix A. Briefly, the trial free energy is minimized and an equation (A18) is derived which relates the chemical-potential difference Δ [Eq. (2.6e)]

to the composition x and the order parameter M [we study here solutions with $Q=0$, Eq. (A8)]. For low temperatures, it is found that there is one special value of Δ , Δ_f , at which the trial free-energy function has three simultaneous minima. Two are at $x = x_M(T)$ with $M = \pm M_0$ [where M_0 is the solution of Eq. (2.9) for $x = x_M(T)$]. The other minimum is at $M=0$ and $x = x_0(T)$. These solutions thus represent the phase separation of a GaAs-rich zinc-blende phase from a Ge-rich diamond phase, shown in Figs. 3 and 4 for low temperatures. Similarly, equilibrium phase separation of a Ge-rich disordered phase from a GaAs-rich *disordered* phase (as shown in Fig. 4) is found by searching for a value of the chemical-potential difference Δ at which two simultaneous minima of the trial free-energy function are found: one each at $x = x_1(T)$ and $x = x_2(T)$, both solutions found for $M=0$. Of course, application of mean-field theory to the *metastable* alloy specifies that such solutions be ignored. That is, the system does not have sufficient time to sense that solutions $x_M(T) \leq x \leq x_0(T)$ or $x_1(T) \leq x \leq x_2(T)$ are to be found for identical values of Δ . Thus, only Eq. (2.9) is of interest in the case of the metastable alloy.

III. CALCULATION OF BAND STRUCTURE FROM MODIFIED VIRTUAL-CRYSTAL APPROXIMATION

The spin-Hamiltonian model [Eq. (2.5)] provides a simple means for minimizing the total free energy of the system and for determining the order parameter $M(x)$. It is, however, ill suited for the computation of electronic structure or optical spectra. For example, the important parameters of the phase-transition model are the differences in the energies of interaction of various nearest neighbors, such as $J_{\text{Ga-Ge}}$ vs $J_{\text{Ga-As}}$. But, for electronic structure, the on-site terms of the Hamiltonian are of greatest importance. This is illustrated by the empirical tight-binding models for band structure, which have nearest-neighbor interactions nearly equal for all semiconductors with similar lattice constants.¹⁷ Thus, if we are to predict the band gap $E_0(x)$ for $(\text{GaAs})_{1-x}\text{Ge}_{2x}$, we must develop a bridge between our total-energy phase-transition model and a model of the band structure. We do this by developing a modified virtual-crystal approximation for the band structure of the metastable alloy, which depends on the order parameter $M(x)$.

In the virtual-crystal approximation, the matrix elements of the tight-binding Hamiltonian are simply interpolated as functions of alloy composition x . For example, the "Ga"-site (cation-site) diagonal matrix element of s symmetry is an average of the

corresponding matrix elements for the constituents:

$$\begin{aligned} E(s; \text{"Ga"}) &= \langle P_{\text{Ga}} \rangle_{\text{"Ga"}} E(s, \text{Ga}; \text{GaAs}) \\ &+ \langle P_{\text{Ge}} \rangle_{\text{"Ga"}} E(s, \text{Ge}; \text{Ge}) \\ &+ \langle P_{\text{As}} \rangle_{\text{"Ga"}} E(s, \text{As}; \text{GaAs}). \end{aligned} \quad (3.1)$$

In the *conventional* virtual-crystal approximation¹⁸ for $(\text{GaAs})_{1-x}\text{Ge}_{2x}$, we have

$$\begin{aligned} \langle P_{\text{Ga}} \rangle_{\text{"Ga"}} &= 1-x, \\ \langle P_{\text{Ge}} \rangle_{\text{"Ga"}} &= x, \end{aligned} \quad (3.2)$$

and

$$\langle P_{\text{As}} \rangle_{\text{"Ga"}} = 0.$$

This approximation is based on the assumption that antisite defects (e.g., As on a Ga site) rarely occur. However, in all the metastable alloys considered here, antisite defects occur in high concentrations. Hence, a *generalized virtual-crystal approximation* is needed. We simply modify the conventional virtual-crystal approximation, Eq. (3.1), by taking the values of Table I, instead of those of Eq. (3.2), making occupation probabilities such as $\langle P_{\text{Ga}} \rangle$ depend on the order parameter $M(x)$:

$$\begin{aligned} \langle P_{\text{Ga}} \rangle_{\text{"Ga"}} &= (1-x+M)/2, \\ \langle P_{\text{Ge}} \rangle_{\text{"Ga"}} &= x, \end{aligned} \quad (3.3)$$

and

$$\langle P_{\text{As}} \rangle_{\text{"Ga"}} = (1-x-M)/2.$$

This prescription accounts for the antisite defects omitted in the conventional virtual-crystal approximation, is (in retrospect) intuitively obvious, and is justified by the algebra of the spin Hamiltonian, Eqs. (A3) to (A8). With it, we have the needed bridge between the spin-Hamiltonian total-energy model and the virtual-crystal empirical tight-binding Hamiltonian of band structure.

For the materials considered here, a generalized virtual-crystal approximation to the electronic structure should be adequate. For III-V and group-IV semiconductive alloys, the differences in the diagonal tight-binding matrix elements of the constituents (e.g., $|E(s, \text{Ga}) - E(s, \text{Ge})|$) are small in comparison with typical nearest-neighbor transfer-matrix elements [e.g., $V(s, s)$]. (See Table II.) Therefore, these materials are in the "amalgamated" regime of alloy theory^{19,26} for which the virtual-crystal approximation provides an adequate theoretical starting point. In the amalgamated regime, the density-of-states spectrum of $(\text{GaAs})_{1-x}\text{Ge}_{2x}$ is expected to be characteristic of a single "average" semiconductor, rather than exhibiting separate GaAs-like or Ge-like

features. Thus, taking the nature of the average anions and cations in $(\text{GaAs})_{1-x}\text{Ge}_{2x}$ from Table I, we have a tight-binding Hamiltonian and a theory of the energy-band structure which depends on the order parameter $M(x)$. The resulting band structure exhibits singularities corresponding to the singularity of $M(x)$ at x_c .

To compute the band structure, we use the Vogl nearest-neighbor empirical sp^3s^* tight-binding theory,¹⁷ but modify it to include some second-neighbor interactions²⁷ while retaining its fit to the band structure determined by Chelikowsky and Cohen.²⁸ The Vogl model is a ten-band model with five basis orbitals per atom (s , p_x , p_y , p_z , and s^* , where s^* is an excited s state). It treats only nearest-neighbor interactions, and its parameters for GaAs and Ge have been fixed so that the model reproduces the band structures at the principle symmetry points Γ [$k=(0,0,0)$] and X [$k=(2\pi/a_L)(1,0,0)$, where a_L is the lattice constant] of the Brillouin zone. The conduction-band minima of Ge are at the L points, $(2\pi/a_L)(\frac{1}{2}, \frac{1}{2}, \frac{1}{2})$, and so we improved the model at point L by adding the second-neighbor parameters ϵ of Table II.²⁷

Within this model, E_0 , the direct band gap at point Γ , is

$$\begin{aligned} E_0 &= \bar{E}_s + [D_s^2 + V^2(s, s)]^{1/2} \\ &- \bar{E}_p + [D_p^2 + V^2(x, x)]^{1/2}. \end{aligned} \quad (3.4)$$

Here we have for GaAs,

$$\begin{aligned} \bar{E}_s &= [E(s, \text{Ga}) + E(s, \text{As})]/2, \\ \bar{E}_p &= [E(p, \text{Ga}) + E(p, \text{As})]/2, \\ D_s &= [E(s, \text{Ga}) - E(s, \text{As})]/2, \end{aligned} \quad (3.5)$$

and

$$D_p = [E(p, \text{Ga}) - E(p, \text{As})]/2.$$

For Ge, we replace Ga and As by Ge in Eqs. (3.5). Here, for example, $E(p, \text{As})$ is the on-site energy in the solid of p symmetry, and $V(s, s)$ and $V(x, x)$ are nearest-neighbor matrix elements between s and p states, respectively.

In the metastable alloy, we interpolate the diagonal matrix elements E according to the generalized *mean-field* virtual-crystal rule, Eqs. (3.1) and (3.3), with the order parameter M given by the mean-field theory, Eq. (2.11). Similar rules are used for interpolating the square of the bond length d times the off-diagonal matrix elements V and ϵ (see Appendix B).

The V -shaped "bowing" of $E_0(x)$ (see Fig. 1) follows from Eq. (3.4), which for $(\text{GaAs})_{1-x}\text{Ge}_{2x}$ predicts $dE_0/dx < 0$ for $x < x_c$ and $dE_0/dx > 0$ for

$x > x_c$. This can be seen by noting that we have $M=0$ for $x > x_c$ in the Ge-rich virtual-diamond (disordered) phase: thus we have $E(s, \text{“Ga”}) = E(s, \text{“As”})$. That is, D_s and D_p in Eqs. (3.4) and (3.5) are zero, and we cannot distinguish anion from cation sites. For $x < x_c$, we have $M \neq 0$, and $E(s, \text{“Ga”}) \neq E(s, \text{“As”})$. The phase is ordered and the anion and cation sites are distinct.

Note that the predicted band gap for GaAs in Fig. 1 is smaller than the usual zero-temperature gap of the tight-binding theory, 1.52 eV.^{17,28} This is because the predictions of Fig. 1 correspond to *metastable* alloys grown at an unknown effective sample-preparation temperature T_{eff} (due to ion bombardment of the samples during growth), and therefore involve materials with $|M(x=0)| \simeq 0.8 < 1$, i.e., there are many antisite defects, such as As on Ga sites. Thus the theory predicts that the band gap of sputter-produced metastable GaAs is smaller than the gap of fully annealed material. Additionally, note that the *square-root* singularity of $M(x)$ (Fig. 7) is an artifact of the mean-field approximation; renormalization-group calculations would obtain for x near x_c a singularity of the form $|M(x)| \sim (x_c - x)^\beta$, with $\beta = 0.325$.²⁹

Results for the conduction-band edge, relative to the valence-band maximum, at Γ_1^C , L_1^C , X_1^C , and X_3^C are given in Fig. 5. Comparing with Fig. 6 for the conventional virtual-crystal approximation, we note several important changes due to the phase transition. First, the splitting in X_1^C and X_3^C due to the distinct anion and cation sites, disappears at the transition point x_c because well-defined anions and cations do not exist in the disordered phase, $x > x_c$. Second, L_1^C shows a similar behavior to Γ_1^C at the transition point, x_c , and crosses with Γ_1^C at $x \simeq 0.75$. This means that the crystalline alloy has a direct gap at Γ for $x < 0.75$ and an indirect gap at L for $x > 0.75$. The band gap thus has *two kinks* as a function of x : one at $x_c = 0.3$, due to the phase transition, and one at $x = 0.75$, due to the crossing of Γ_1^C with L_1^C . We emphasize that the observed kink or *V-shaped bowing* at $x_c \simeq 0.3$ is due to the phase transition and not to the Γ_1^C - L_1^C direct-indirect crossover of the conduction-band structure.

Finally, we exhibit the density of electronic states (Fig. 8) calculated for $(\text{GaAs})_{1-x}\text{Ge}_{2x}$ alloys, in the hopes of stimulating independent experimental tests of the proposed phase-transition model. These densities of states were calculated using the Lehmann-Taut method³⁰ for the tight-binding model, and should be especially reliable for the valence bands. Some features of the conduction bands, especially those above 6 eV, are unphysical (and the price to be paid for obtaining a simple two-neighbor tight-

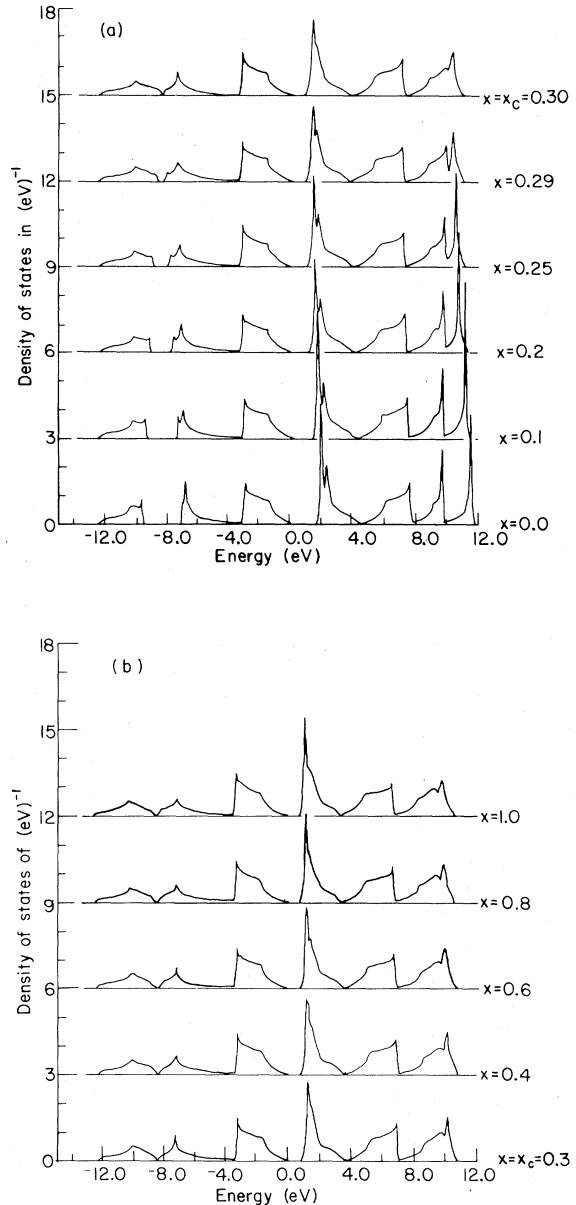


FIG. 8. Density of states $[(\text{eV})^{-1}]$ vs energy E (eV) for $(\text{GaAs})_{1-x}\text{Ge}_{2x}$. (a) For $x = 0, 0.1, 0.2, 0.25,$ and $0.29,$ and $x_c = 0.3$ and (b) for $x = x_c = 0.3, 0.4, 0.6, 0.8,$ and 1.0 . Note that the gap at approximately -8 eV disappears as x approaches x_c . The calculation uses an empirical tight-binding sp^3s^* band structure (Ref. 17), and thus is quantitatively reliable for $E < 0$, and semiquantitatively reliable only for the lowest of the conduction bands. Nevertheless, for completeness, we include the features for $E > 6$ eV.

binding description of a complex band structure).

The most prominent feature of these state densities is the gap at approximately -8 eV in GaAs

(characteristic of III-V compounds) which suddenly fills in for x near x_c , producing the characteristic triangular diamond-structure density of states. This filling occurs because the distinction between anions and cations is suddenly lost for $x = x_c$; there is no splitting of X_1 and X_3 for $x > x_c$ (see also Fig. 5). Note also the disappearance of sharp features present for $x=0$ as $x \rightarrow x_c$. This is a result of the phase transition, and *not* of alloy broadening (which is not taken into account in the present theory). We hope that experiments will be performed to determine if $(\text{GaAs})_{1-x}\text{Ge}_{2x}$ alloys suddenly lose the gap at -8 eV in their densities of states, as x approaches x_c .

IV. CONCLUSIONS

We have proposed a new type of phase transition, from an ordered GaAs-rich zinc-blende structure ($x < x_c$) to a disordered Ge-rich diamond structure ($x > x_c$), as an explanation of the anomalous dependence on alloy composition x of the direct band gap $E_0(x)$ of $(\text{GaAs})_{1-x}\text{Ge}_{2x}$. The order parameter of the phase transition $M(x)$, is evaluated in a mean-field approximation, using a three-component "antiferromagnetic" spin model, in which spins "up," "zero," and "down" on a site represent occupation by Ga, Ge, and As atoms. The nonequilibrium nature of the alloys is accounted for by excluding thermodynamic states corresponding to phase separation, which cannot be achieved during the growth process. The order parameter obtained using mean-field theory is then inserted into an empirical tight-binding model of electronic structure, which is evaluated using a new generalized mean-field virtual-crystal approximation to the band structure, Eqs. (3.1) and (3.3). The resulting band edges (Fig. 5) exhibit "kinks" as functions of alloy composition, which reflect the critical singularity of the order parameter. The predicted band edge $E_0(x)$ is in good agreement with the data (Fig. 1). Finally, the theory offers a first crude step²² toward first-principles calculation of the phase diagrams of new metastable crystalline alloys such as $(\text{GaAs})_{1-x}\text{Ge}_{2x}$.

ACKNOWLEDGMENTS

We wish to thank A. C. Redfield and B. A. Bunker for many useful discussions. We are grateful to A. Lastras-Martinez, B. Kramer, and J. E. Greene for extensive discussions of their data. Finally, we thank the U.S. Office of Naval Research (Contract No. N00014-77-C-0537) for their generous financial support.

APPENDIX A

We use a variational method²⁵ to solve approximately (using mean-field theory) for F , Eq. (2.4). The trial free energy, F_t , is given by

$$F_t = \text{Tr}(H\rho_t) + k_B T \text{Tr}(\rho_t \ln \rho_t) \quad (\text{A1})$$

where ρ_t is a trial density matrix that satisfies

$$\text{Tr}\rho_t = 1 .$$

For each sublattice ("Ga" and "As"), we define separate density matrices,

$$\begin{aligned} \rho_1 &= [\exp(\alpha S_1 + \beta S_1^2)] / Z_1 , \\ \rho_2 &= [\exp(\delta S_2 + \gamma S_2^2)] / Z_2 . \end{aligned} \quad (\text{A2})$$

Here S_1 and S_2 sit on the "Ga" and "As" sublattices, respectively; therefore,

$$\rho_t = \prod_i \rho_i = \rho_1^{N/2} \rho_2^{N/2} .$$

In terms of the spin variables, we define the following average sublattice occupancies:

$$\begin{aligned} m_{\text{"Ga"}} &= \langle S_i \rangle_{\text{"Ga"}} , \\ m_{\text{"As"}} &= \langle S_i \rangle_{\text{"As"}} , \\ q_{\text{"Ga"}} &= \langle S_i^2 \rangle_{\text{"Ga"}} , \end{aligned} \quad (\text{A3})$$

and

$$q_{\text{"As"}} = \langle S_i^2 \rangle_{\text{"As"}} .$$

Equations (A3) can be used to find expressions for the average occupancies [Eqs. (2.1)] of each type of atom on each type of site; for the "Ga" site, we find

$$\begin{aligned} \langle P_{\text{Ga}} \rangle_{\text{"Ga"}} &= (q_{\text{"Ga"}} + m_{\text{"Ga"}}) / 2 , \\ \langle P_{\text{Ge}} \rangle_{\text{"Ga"}} &= 1 - q_{\text{"Ga"}} , \end{aligned} \quad (\text{A4})$$

and

$$\langle P_{\text{As}} \rangle_{\text{"Ga"}} = (q_{\text{"Ga"}} - m_{\text{"Ga"}}) / 2 .$$

In terms of definitions (A3), using Eq. (2.8), the order parameter M is

$$2M = m_{\text{"Ga"}} - m_{\text{"As"}} . \quad (\text{A5})$$

Definitions (A3) are useful also for expressing mathematically the constraint that we study the material $(\text{GaAs})_{1-x}\text{Ge}_{2x}$. First, since there are equal numbers of Ga ($S = +1$) and As ($S = -1$) atoms, using Eqs. (2.1) we find

$$m_{\text{"Ga"}} + m_{\text{"As"}} = 0 , \quad (\text{A6})$$

that is, the average of the spin variable S over the entire system must be zero. Second, since a fraction

$1-x$ of spins S represent GaAs ($S = \pm 1$), the composition x is given by

$$q_{\text{Ga}} + q_{\text{As}} = 2(1-x). \quad (\text{A7})$$

Finally, it is possible to imagine *another* type of order parameter, Q :

$$2Q \equiv q_{\text{Ga}} - q_{\text{As}}, \quad (\text{A8})$$

that measures the tendency of Ga and As atoms to be adjacent to Ge atoms. For this paper, since we have $J + K > 0$, Eq. (2.7), we assume $Q = 0$. Then, using Eqs. (A5) to (A8), Eqs. (A4) reduce to the results of Table I.

For the trial free energy, assuming $L = 0$, we find

$$\begin{aligned} F_t/N = & Jzm_{\text{Ga}}m_{\text{As}}/2 - Kzq_{\text{Ga}}q_{\text{As}}/2 + \Delta(q_{\text{Ga}} + q_{\text{As}})/2 + h(m_{\text{Ga}} + m_{\text{As}}) \\ & + k_B T [\alpha m_{\text{Ga}} + \beta q_{\text{Ga}} - \ln Z_{\text{Ga}} + \delta m_{\text{As}} + \gamma q_{\text{As}} - \ln Z_{\text{As}}]/2 \end{aligned} \quad (\text{A9})$$

where N is the total number of sites and we have [from Eqs. (A2) and (A3)]

$$\begin{aligned} m_{\text{Ga}} &= \frac{2 \sinh \alpha}{e^{-\beta} + 2 \cosh \alpha}, \\ m_{\text{As}} &= \frac{2 \sinh \delta}{e^{-\gamma} + 2 \cosh \delta}, \\ q_{\text{Ga}} &= \frac{2 \cosh \alpha}{e^{-\beta} + 2 \cosh \alpha}, \end{aligned} \quad (\text{A10})$$

and

$$q_{\text{As}} = \frac{2 \cosh \delta}{e^{-\gamma} + 2 \cosh \delta}.$$

Minimizing (A9) with respect to m_{Ga} , m_{As} , q_{Ga} , q_{As} , and using Eqs. (A5) to (A8), we find

$$h = -k_B T(\alpha + \delta)/4, \quad (\text{A11})$$

$$2JzM/(k_B T) = \alpha - \delta, \quad (\text{A12})$$

$$2KzQ/(k_B T) = \gamma - \beta, \quad (\text{A13})$$

and

$$2[-\Delta + Kz(1-x)]/(k_B T) = \beta + \gamma. \quad (\text{A14})$$

Equations (A11) to (A14) are similar to those derived for binary alloys.²² Using Eqs. (A10) and (A5) to (A8), we can find expressions for α , β , γ , and δ in terms of M , Q , and x . Equations (A11) to (A14) can then be written as follows:

$$\frac{8h}{k_B T} = \ln \frac{(1-x)^2 - (Q-M)^2}{(1-x)^2 - (Q+M)^2}, \quad (\text{A15})$$

$$\frac{4JzM}{k_B T} = \ln \frac{(1-x+Q+M)(1-x-Q+M)}{(1-x+Q-M)(1-x-Q-M)}, \quad (\text{A16})$$

$$\frac{4JzM}{k_B T} = \ln \frac{(1-x+Q+M)(1-x-Q+M)}{(1-x+Q-M)(1-x-Q-M)}, \quad (\text{A17})$$

and

$$4[\Delta - Kz(1-x)]/(k_B T) = -\ln \{ [(1-x+Q)^2 - M^2][(1-x-Q)^2 - M^2] \} + 2 \ln [4(x^2 - Q^2)]. \quad (\text{A18})$$

Solution of these equations for Q , x , and M as functions of h , Δ , and T for given values of J and K yields information about the equilibrium phase diagrams of $(\text{GaAs})_{1-x}\text{Ge}_{2x}$.

Solution of Eqs. (A15) and (A18) for phase boundaries proceeds as outlined in Ref. 20. [Here, we take $Q = 0$; thus $h = 0$ in Eq. (A15).] We summarize some useful formulas. First we find from Eq. (A16) the order-disorder critical line, Eq. (2.10). Then, as described in Ref. 20, using definitions

$$R \equiv K/J \quad (\text{A19})$$

and

$$\tau \equiv k_B T/(Jz),$$

the location of the tricritical point (τ_t, x_t) is found as follows:

$$1 - x_t = \tau_t = \frac{1 + 2R}{3 + 2R}. \quad (\text{A20})$$

For $\tau < \tau_t$, either three- or four-phase separation [see Refs. 20 and 31] is possible—this is searched for numerically, using Eqs. (A16) and (A18). The possibility of two-phase separation is studied using a new variable, u :

$$u \equiv 1 - 2x. \quad (\text{A21})$$

To find the two-phase-separation critical point, $(\tau_{\text{crit}}, x_{\text{crit}})$ (see Fig. 4), Eq. (A18) is rewritten (for $M = Q = 0$):

$$u = \frac{1 - \exp[-\ln 2 + \Delta/(k_B T) - R(1+u)/(2\tau)]}{1 + \exp[-\ln 2 + \Delta/(k_B T) - R(1+u)/(2\tau)]}. \quad (\text{A22})$$

We thus see that there is an effective "magnetic field," h_{eff} ,

$$h_{\text{eff}} = -\ln 2 + \Delta/k_B T - R/(2\tau), \quad (\text{A23})$$

which must be set to zero to see the transition (this is the Griffiths' symmetry, Ref. 32). For $h_{\text{eff}}=0$, Eq. (A22) may be written [in a form analogous to Eq. (2.9)],

$$u = \tanh \frac{Ru}{4\tau}. \quad (\text{A24})$$

The phase-separation critical point is thus at $u=0$, $\tau_{\text{crit}}=R/4$, or $(\tau_{\text{crit}}, x_{\text{crit}})=(R/4, 1/2)$. Numerical solution of Eq. (A24) for $\tau < \tau_{\text{crit}}$ determines [using Eq. (A21)] $x_1(\tau)$ and $x_2(\tau)$ (as shown in Fig. 4). The intersection of the critical line, Eq. (2.10), with this phase-separation line (see Fig. 4) occurs at a critical end point: (x_3, τ_3) , where τ_3 is the solution to

$$(2\tau_3 - 1) = \tanh \frac{R(2\tau_3 - 1)}{4\tau_3}. \quad (\text{A25})$$

$$\begin{aligned} V(s,s;(\text{GaAs})_{1-x}\text{Ge}_{2x})d^2 = & [\langle P_{\text{Ga}}(1)P_{\text{As}}(2) \rangle + \langle P_{\text{As}}(1)P_{\text{Ga}}(2) \rangle]V(s,s;\text{GaAs})d_{\text{Ga-As}}^2 \\ & + \langle P_{\text{Ge}}(1)P_{\text{Ge}}(2) \rangle V(s,s;\text{GeGe})d_{\text{Ge-Ge}}^2 + \langle P_{\text{Ga}}(1)P_{\text{Ga}}(2) \rangle V(s,s;\text{GaGa})d_{\text{Ga-Ga}}^2 \\ & + \langle P_{\text{As}}(1)P_{\text{As}}(2) \rangle V(s,s;\text{AsAs})d_{\text{As-As}}^2 \\ & + [\langle P_{\text{Ge}}(1)P_{\text{As}}(2) \rangle + \langle P_{\text{As}}(1)P_{\text{Ge}}(2) \rangle]V(s,s;\text{GeAs})d_{\text{Ge-As}}^2 \\ & + [\langle P_{\text{Ga}}(1)P_{\text{Ge}}(2) \rangle + \langle P_{\text{Ge}}(1)P_{\text{Ga}}(2) \rangle]V(s,s;\text{GaGe})d_{\text{Ga-Ge}}^2. \end{aligned} \quad (\text{B2})$$

(Here, 1 is a "Ga" site; 2 is a neighboring "As" site.) Since matrix elements such as $V(s,s;\text{GeAs})$ are not known, we make the following simple approximation. For $V(s,s;\text{GaGa})d_{\text{Ga-Ga}}^2$ and $V(s,s;\text{AsAs})d_{\text{As-As}}^2$, we use simply $V(s,s;\text{GaAs})d_{\text{Ga-As}}^2$. For $V(s,s;\text{GeAs})d_{\text{Ge-As}}^2$ and $V(s,s;\text{GaGe})d_{\text{Ga-Ge}}^2$, we use an average, e.g.,

$$\begin{aligned} V(s,s;\text{GeAs})d_{\text{Ge-As}}^2 = & [V(s,s;\text{GaAs})d_{\text{Ga-As}}^2 \\ & + V(s,s;\text{GeGe})d_{\text{Ge-Ge}}^2]/2. \end{aligned} \quad (\text{B3})$$

Joint-occupancy probabilities are expressible in terms of spin-spin correlation functions. These are trivially found for the mean-field approximation (nontrivial corrections will come from a more sophisticated treatment): For example, using Eq. (A2),

For phase diagrams determined for other values of R from mean-field theory, see Ref. 20.

APPENDIX B

The mean-field virtual-crystal estimates for the variation with x of the off-diagonal matrix elements V and ϵ of Table II are obtained as follows. First, the bond length d is determined by Vegard's law, i.e., d is linearly interpolated as a function of x :

$$d = (1-x)d_{\text{Ga-As}} + xd_{\text{Ge-Ge}}. \quad (\text{B1})$$

We then interpolate combinations Vd^2 and ϵd^2 using joint-occupancy probabilities such as $\langle P_{\text{Ga}}(i)P_{\text{As}}(j) \rangle$, where i and j label atomic sites (e.g., for V , i labels the central atom and j denotes its neighbor, and for ϵ , j denotes a second-neighbor position). (Actually, since GaAs and Ge are well lattice-matched, interpolating Vd^2 or ϵd^2 is essentially the same as interpolating V or ϵ .) Here, since the order parameter Q of Eq. (A8) is zero, we have joint occupancy probabilities that are symmetric under interchange of i and j . For $V(s,s;(\text{GaAs})_{1-x}\text{Ge}_{2x})$, for example, we find

we find

$$\langle S_i S_j \rangle_{\text{"Ga"}, \text{"As"}} = \langle S_i \rangle_{\text{"Ga"}} \langle S_j \rangle_{\text{"As"}}. \quad (\text{B4})$$

Then, Eqs. (B3) and (B4) allow a great simplification to Eq. (3.2):

$$\begin{aligned} V(s,s;(\text{GaAs})_{1-x}\text{Ge}_{2x})d^2 = & (1-x)V(s,s;\text{GaAs})d_{\text{Ga-As}}^2 \\ & + xV(s,s;\text{GeGe})d_{\text{Ge-Ge}}^2. \end{aligned} \quad (\text{B5})$$

For matrix elements such as $V(sc,pa)$ and $V(sa,pc)$, we make the following type of prescriptions for the unknown matrix elements:

$$\begin{aligned} V(pc,sa;\text{GaGe})d_{\text{Ga-Ge}}^2 = & [V(pc,sa;\text{GaAs})d_{\text{Ga-As}}^2 \\ & + V(pc,sa;\text{GeGe})d_{\text{Ge-Ge}}^2]/2, \end{aligned} \quad (\text{B6})$$

$$V(pa,sc;GaGe)d_{Ga-Ge}^2 \\ = [V(pa,sc;GaAs)d_{Ga-As}^2 \\ + V(pa,sc;GeGe)d_{Ge-Ge}^2]/2, \quad (B7)$$

and

$$V(pc,sa;AsAs)d_{As-As}^2 \\ = [V(pc,sa;GaAs)d_{Ga-As}^2 \\ + V(pa,sc;GaAs)d_{Ga-As}^2]/2. \quad (B8)$$

In Eq. (B6), we have a Ga atom on a "Ga" (*c* or cation), while in Eq. (B7), Ga sits on the "As" (*a* or

anion) site. With approximations of this type, we find matrix elements $V(sc,pa;(GaAs)_{1-x}Ge_{2x})$ and $V(sa,pc;(GaAs)_{1-x}Ge_{2x})$ to have the same form as Eqs. (3.1) and (3.3), e.g.,

$$V(sa,pc;(GaAs)_{1-x}(Ge_2)_x)d^2 \\ = (1-x+M)V(sa,pc;GaAs)d_{Ga-As}^2/2 \\ + (1-x-M)V(sc,pa;GaAs)d_{Ga-As}^2/2 \\ + xV(sa,pc;GeGe)d_{Ge-Ge}^2. \quad (B9)$$

All other matrix elements are determined in an analogous fashion.

¹For a review, see J. E. Greene and A. H. Eltoukhy, *Surf. Interface Anal.* **3**, 34 (1981).

²S. A. Barnett, M. A. Ray, A. Lastras, B. Kramer, J. E. Greene, P. M. Raccah, and L. L. Abels, *Electron. Lett.* **18**, 891 (1982).

³K. C. Cadien, A. H. Eltoukhy, and J. E. Greene, *Appl. Phys. Lett.* **38**, 773 (1981); *Vacuum* **31**, 253 (1981).

⁴K. E. Newman, A. Lastras, B. Kramer, S. A. Barnett, M. A. Ray, J. D. Dow, J. E. Greene, and P. M. Raccah, *Phys. Rev. Lett.* (in press).

⁵For a discussion of the general theory of order-disorder phase transitions, see E. M. Lifshitz and L. P. Pitaevskii, *Statistical Physics*, Part 1 (Pergamon, Oxford, 1980).

⁶For a treatment of semiconductors that have zinc-blende or diamond lattices, see W. A. Harrison, *Electronic Structure and Properties of Solids* (Freeman, San Francisco, 1980).

⁷The theory is actually applicable to all alloys of materials $(CA)_{1-x}D_{2x}$, where material *D* is of the same structure as material *CA*, but has nominal anions (*A*) and cations (*C*) that are the same.

⁸A more general definition of *M* is found in Sec. II [Eq. (2.8)] that is the average of Eqs. (1.1) and (1.2). For the range of parameters of the model that we study here, all three definitions are equivalent. If phases GaGe and GeAs are to be studied, then Eq. (2.8) only should be used.

⁹A. J. Noreika and M. H. Francombe, *J. Appl. Phys.* **45**, 3690 (1974).

¹⁰K. C. Cadien and J. E. Greene, *Appl. Phys. Lett.* **40**, 329 (1981).

¹¹L. Romano, S. Fang, and J. E. Greene (unpublished).

¹²The lifetime of $(GaAs)_{1-x}Ge_{2x}$ is estimated to be similar to that obtained for $(GaSb)_{1-x}Ge_{2x}$. It may, in fact, be considerably shorter for $x \rightarrow 0, 1$.

¹³Electron-microscopy studies imply that domains must be less than 30 Å in size (see Ref. 4).

¹⁴D. L. Kendall, *Semiconductors and Semimetals*, edited by R. K. Willardson and A. C. Beer (Academic, New York, 1968), Vol. 4.

¹⁵The diffusion constant *D* has a form $D = D_0 \exp[-Q/(k_B T)]$. For As self-diffusion in GaAs (Ref. 14), $D_0 = 0.7 \text{ cm}^2 \text{ s}^{-1}$ and $Q = -3.2 \text{ eV}$. Assuming isotropic dispersion, we find the mean-square distance *r* traveled in a time *t* is given by $\langle r^2 \rangle = 6D_0 t$. Thus, on the average, there will be a factor-of-100 difference in the time to diffuse 3 vs 30 Å.

¹⁶R. B. Griffiths, *Phys. Rev. Lett.* **24**, 715 (1970).

¹⁷P. Vogl, H. P. Hjalmarsen, and J. D. Dow, *J. Phys. Chem. Solids* (in press).

¹⁸In the virtual-crystal model, the nominal cation and anion sites are assumed to be occupied by "Ga_{1-x}Ge_x" and "As_{1-x}Ge_x" atoms, respectively. See, for example, R. H. Parmenter, *Phys. Rev.* **97**, 587 (1955).

¹⁹C. W. Myles and J. D. Dow, *Phys. Rev. B* **19**, 4939 (1979).

²⁰M. Blume, V. J. Emery, and R. B. Griffiths, *Phys. Rev. A* **4**, 1071 (1971).

²¹J. Sivardière and J. Lajzerowicz, *Phys. Rev. A* **11**, 2079 (1975); **11**, 2090 (1975); **11**, 2101 (1975).

²²For another attempt at calculation of alloy phase diagrams, see V. Saito, *J. Chem. Phys.* **74**, 713 (1981).

²³ $(GaAs)_{1-x}Ge_{2x}$ alloys could, instead, be modeled as a "ferromagnet" having three components: GaAs molecules on a face-centered-cubic lattice and which are diluted by Ge₂ molecules of spin "0". We choose to study the atomic antiferromagnetic model of the alloy because it is simpler and because only that model allows the possibility of GeAs and GaGe phases.

²⁴There is indeed a compound GeAs (and, also GeAs₂), but it has a very different (layered) lattice structure. See, for example, W. B. Pearson, *The Crystal Chemistry and Physics of Metals and Alloys* (Wiley-Interscience, New York, 1972).

²⁵H. Falk, *Am. J. Phys.* **30**, 858 (1970).

²⁶Y. Onodera and Y. Toyozawa, *J. Phys. Soc. Jpn.* **24**, 341 (1968).

²⁷K. E. Newman and J. D. Dow (unpublished).

²⁸J. R. Chelikowsky and M. L. Cohen, *Phys. Rev. B* **14**, 556 (1976).

²⁹J. C. Le Guillou and J. Zinn-Justin, *Phys. Rev. B* **21**,

- 3976 (1980).
- ³⁰G. Lehmann and M. Taut, *Phys. Status Solidi B* 54, 469 (1972).
- ³¹Some features of the Blume-Emery-Griffiths phase diagram (Ref. 20), such as a four-phase coexistence point for $J/K = 2.88$, are not seen in phase diagrams determined using renormalization-group theory. See, for example, A. N. Berker and M. Wortis, *Phys. Rev. B* 14, 4946 (1976); M. Kaufman, R. B. Griffiths, J. M. Yeomans, and M. E. Fisher, *Phys. Rev. B* 23, 3448 (1981); J. M. Yeomans and M. E. Fisher, *Phys. Rev. B* 24, 2825 (1981).
- ³²R. B. Griffiths, *Physica* 33, 689 (1967).